Configuration and Site of O_2 Adsorption on the Pt(111) Electrode Surface

R. R. Adžić* and J. X. Wang

Chemical Sciences Division, Department of Applied Science, Brookhaven National Laboratory, Upton, New York 11973

Received: February 11, 1998; In Final Form: July 15, 1998

The inhibition of O_2 reduction on a Pt(111) electrode surface with Ag adatoms has been studied to gain information on the type of O_2 adsorption during the reaction. A pronounced inhibition is observed upon adsorption of Ag submonolayers, and a complete inhibition is caused by underpotential deposition of a pseudomorphic Ag monolayer and of an incommensurate hexagonal bilayer. Electrochemical and in situ surface X-ray scattering techniques were used to obtain kinetic and structural data. Statistical models for the inhibition of O_2 reduction caused at submonolayers of Ag adatoms residing on top, bridge, and hollow sites of Pt(111) for O_2 adsorbed on the same type of sites in three different configurations have been compared with the experimental data. Analysis of the extent of the inhibition of O_2 reduction as a function of the Ag coverage shows that the data are best interpreted with O_2 adsorbed at a bridge site.

Introduction

The type of O_2 interaction with electrode surfaces has been a long-standing question of oxygen electrocatalysis. There is no experimental data about the site and configuration of O_2 adsorbed on an electrode surface, which is critical for the first stage of its reduction. This is caused by a lack of techniques capable of revealing information on the relatively weakly interacting molecular oxygen with the surface atoms. Consequently, no distinction between the three plausible types of O_2 adsorption, viz., Griffith (on-top, double bond),[1] Pauling (on-top, single bond),[2] and "bridge"[3] could have been made thus far. These types of bonding are well-known in inorganic coordination chemistry. They are also expected to occur for metal surfaces with localized d orbitals, as is the case of platinum group metals. According to these models (Figure 1), O_2 interacts with electrode surfaces in the following ways:

(i) O_2 interacts with a single substrate atom (Griffith model) by forming a bond mainly between its σ orbitals and the empty d_{z^2} orbitals of the metal surface atom, and by forming a σ back-bond from the partially filled d_{xy} or d_{yz} metal orbitals to the antibonding π^* orbitals of O_2.[4]

(ii) End-on adsorption through a single σ type bond (Pauling model), in which the σ orbital of O_2 donates electron density to an acceptor d_z2 orbital on the metal.

(iii) Bridge model, with two bonds with two sites, which was proposed by Yeager[3] principally for the reaction on platinum group metals.

Oxygen adsorption on clean metal surfaces at the metal−gas interface has been the subject of numerous studies in order to establish the nature of the chemisorption, the bond strength, and the structure of the absorbed layer. Oxygen adsorbs in molecular form at low temperatures, while dissociative adsorption on platinum group metals occurs at temperatures in the range 150−300 K. The system O_2−Pt(111) was investigated with a particularly broad variety of methods. A recent study confirmed the existence of the three types of oxygen adsorbates on Pt(111), viz., physisorbed O_2, at about 25K, chemisorbed,

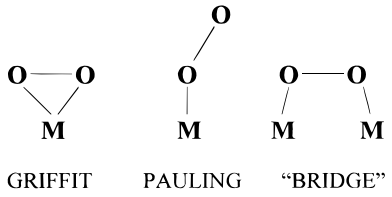

Figure 1. Models of O_2 adsorption on electrode surfaces.[3]

at 90−135K, and an atomic phase above 150K.[5] The electronic structure of a chemisorbed oxygen molecule is strongly perturbed due to the hybridization with the metal substrate. This can be described as a charge transfer from the metal to the molecular $1\sigma_g$ orbital. The peroxo (O_2^{2-}) species was inferred from electron energy loss spectroscopy (EELS)[6] and the superoxo species (O_2^-) was detected by near-edge X-ray absorption spectroscopy (NEXAFS).[7] A bridge-bonded species with an O−O stretching frequency of $\nu = 700$ cm^{-1} and an on-top species with $\nu = 875$ cm^{-1}, both of the peroxo type, were inferred from EELS.[6] Although adsorption of O_2 on a bare and on a water-covered Pt surface can differ substantially, these data can be considered as strong support for reaction schemes for Pt which involve a dissociation of the O_2 molecule in the first step.

The chemisorption of molecular oxygen on a Pt(111) surface was recently examined using tight-binding extended Hückel calculations.[8] It was found that chemisorption of O_2 appears to be more favorable at the 2-fold-bridge site than on on-top or on 3-fold sites. The stabilization is due to the better overlap of the O_2 $2\sigma_u$ orbital with the Pt surface.

In this work, an indirect way of examination of the O_2 adsorption on Pt(111) has been utilized. The inhibition of O_2 reduction on Pt(111) by Ag adatoms was used to obtain information on the configuration O_2 adsorbed on Pt(111) during reduction. Ag forms two monolayers in the underpotential deposition (UPD) on Pt(111).[9−11] Unlike many other metal adatoms that have small or negligible effects on O_2 reduction on Pt,[12] Ag causes a complete inhibition of this reaction. Cu, for example, causes a complete inhibition of O_2 reduction at full monolayer coverage, while at a 2/3 coverage[13] it supports

* Author to whom correspondence should be addressed.

10.1021/jp981057z CCC: $15.00
Published on Web 10/16/1998

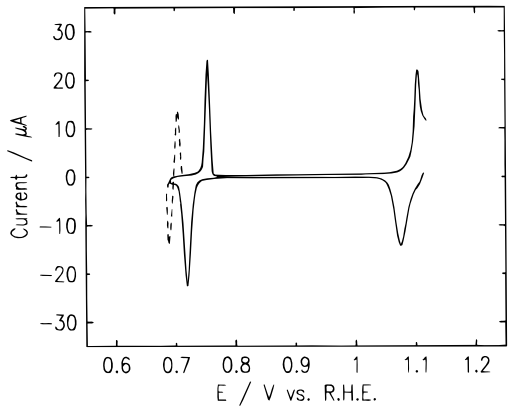

Figure 2. Voltammetry curve for the UPD of Ag on Pt(111) in 0.05 M H_2SO_4 with 2 mM Ag_2SO_4. Sweep rate 2 mV/s.

a 2e-reduction.[14] Ag appears to be unique to cause a large inhibition at small coverages. This inhibition provides a possibility of using Ag adatoms as a probe of adsorption of O_2 on electrode surfaces. The inhibition of O_2 reduction has been measured as a function of the Ag coverage. Surface X-ray scattering (SXS) measurements during the course of reduction were used to show that this reaction does not affect the Ag adlayer structure in the absence of Ag^+ in solution. They confirm that Ag forms a hexagonal incommensurate bilayer, with two mutually commensurate monolayers. The first monolayer has a commensurate, pseudomorphic (1×1) structure, where the Ag atoms reside in the 3-fold symmetry hollow sites on the Pt(111) surface.[15] This fact, in addition to the effect of adsorbed Ag submonolayers on O_2 reduction, has been used as support of the 3-fold symmetry adsorption sites of Ag in the submonolayer range.

Experimental Section

Platinum disks (6 mm × 6 mm, and 10 mm × 3 mm) were aligned, polished, and annealed as previously reported.[15] The electrochemical X-ray scattering cell was described in reference.[16] The solutions were prepared from Ag_2SO_4 or $AgNO_3$ (Aldrich) and H_2SO_4 (SeaStar) and Millipore QC UV Plus water (Millipore Inc.). At a potential slightly positive of Ag deposition potential, the cell was deflated, leaving a thin 10-μm-thick capillary electrolyte film between the Pt(111) face and the Prolene X-ray window. A reversible hydrogen electrode (R.H.E.) in Ag-free solutions was used as a reference electrode. Rotating hanging meniscus electrode measurements were carried out with a crystal 6 mm in diameter, 6 mm long. The rotator (Pine Instrument Co.) was fitted with a collet crystal holder that is similar to the one described earlier.[17]

SXS measurements were carried out at the National Synchrotron Light Source (NSLS) at beam line ×22B with λ = 1.54 Å. A full description of the electrochemical SXS technique has been presented elsewhere.[16] For Pt(111) it is convenient to use a hexagonal coordinate system in which Q = (a*, b*, c*) × (H, K, L), where $a^* = b^* = 4\pi/\sqrt{3}a = 2.614$ Å^{-1}, $c^* = 2\pi/\sqrt{6}a = 0.924$ Å^{-1}, and a = 2.775 Å. The in-plane diffraction measurements were carried out in the (H, K) plane with L = 0.2 corresponding to a grazing angle of 1.25 degrees.

Results and Discussion

Oxygen Reduction on Pt(111)/Ag_{ad}. Figure 2 shows a linear potential voltammetry curve for the UPD of Ag on Pt(111) in 0.05 M H_2SO_4 containing 2 mM Ag^+. Two pronounced peaks in the cathodic sweep at potentials 1.07 and 0.73 V are due to a deposition of two Ag monolayers. The corresponding peaks in the anodic direction occur at 0.76 and 1.1 V. The X-ray diffraction measurements show a formation of a Ag bilayer, with one monolayer associated with each peak. Ag forms a commensurate (1×1) monolayer on Pt(111) by occupying the 3-fold symmetry hollow sites at potentials between the two voltammetry peaks. Deposition of the second Ag adlayer causes a restructuring of the first monolayer. At 0.7 V, negative of the second peak, Ag forms an incommensurate aligned hexagonal bilayer with the lattice constant of 2.952 Å.[15] Figure 3 shows models of side views at the Ag monolayer and bilayer on the Pt(111) surface. From the observed in-plane diffraction pattern, and from the intensity profile of the surface rods, it was found that the two adlayers are mutually commensurate.[15] The Ag bilayer is stable after Ag^+ ions are removed from the solution.

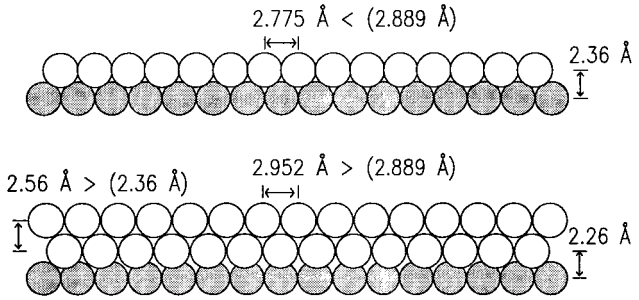

Figure 3. Models for a Ag monolayer and bilayer on Pt(111). Ag (open circles) is 4% larger than Pt (solid circles) in diameter. Lattice spacings of bulk Ag are given in parentheses.

Structural information on the foreign metal adlayers provides a possibility for a more complete study of their electrocatalytic effects on various reactions and their use as a probe of adsorption processes at electrode surfaces. The position of foreign adatoms on the substrate surface can be monitored during the course of a reaction by utilizing in situ SXS technique.[18,19] Some limitations imposed by the cell construction on the supply of reactants, O_2 in this case, into the thin solution film facing the surface being examined were discussed elsewhere.[18] Limitations for O_2 reduction appear to be minor, since it can be brought perpendicular to the surface being investigated by diffusion through a thin Prolene film covering the cell. There is, however, a problem of current distribution. For this cell, the current at the edge of the electrode is certainly larger than the current at the center of the front face of the crystal. This apparently does not cause a problem at small current densities, which is the case with this reaction. It has been shown that the aligned hexagonal structure of the Tl adlayer on Au(111) vanishes with O_2 reduction, but recovers when O_2 is replaced by N_2.[18,19] This indicates that the reaction occurs over the whole front surface of the crystal.

Grazing incident angle X-ray diffraction measurements were performed in order to determine the surface structure of electrodeposited silver adlayers in the presence of O_2 reduction. Figure 4 shows typical in-plane diffraction scans along the K direction at two different potentials and the effect of O_2 on the intensity of the diffraction peak at (0,0.94) position in reciprocal space for the Ag hexagonal bilayer with Ag^+ in solution. A comparison with the measurement at 0.7 V in the absence of O_2 shows a negligible decrease in the diffraction intensity. In the absence of Ag^+ in solution, O_2 reduction occurs at 0.2 V and causes a considerable decrease of the diffraction intensity. The peak position, however, is unchanged, which means that the adlayer structure remains unchanged in the presence of O_2 reduction (Figure 4). The decrease in the diffraction intensity is probably due to a decrease of the ordering of the adlayer,

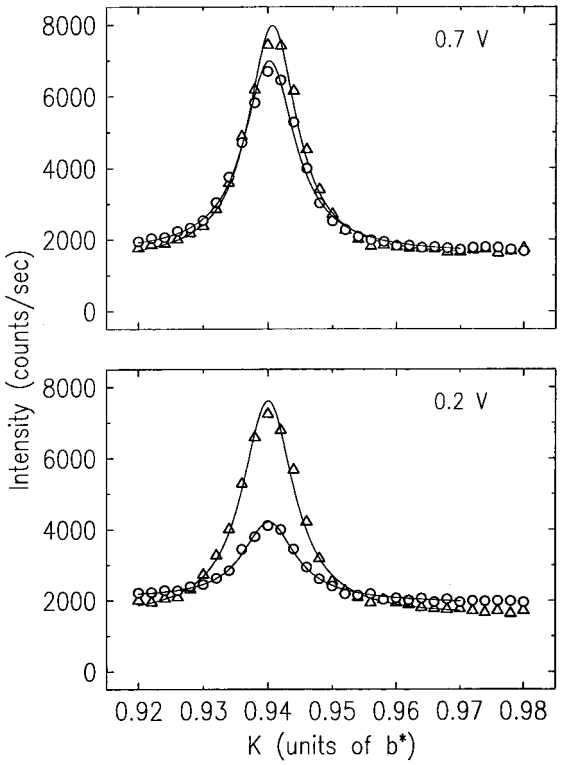

Figure 4. In-plane diffraction scans along the (0,K,0.3) axis from Pt(111) in 0.05 M H_2SO_4 at indicated potentials in the absence (triangles) and in the presence of O_2 reduction (circles). Solid lines are the fits to a Lorenzian line shape.

which is probably caused by the increased vibration of adatoms in the presence of O_2 reduction. A similar decrease of diffraction intensity was observed during O_2 reduction on the hexagonal Tl adlayer on Au (111).[18] Since the structure of the bilayer is not significantly affected by O_2 reduction, the structure of the Ag monolayer should be even less affected since the interaction of Ag adatoms with Pt is stronger for the latter adlayer. The stability and position of Ag adatoms in submonolayers are critical for the analysis of the inhibition as a function of coverage. The stability is easily confirmed by the lasting inhibition effect in the absence of Ag^+ in solution. The data presented below indicate that Ag atoms in submonolayers are in the 3-fold symmetry sites as in the monolayer.

Figure 5 shows O_2 reduction on Pt(111) obtained with a hanging meniscus rotating disk electrode in the absence and in the presence of the Ag adlayers. The curve for Pt(111) is in agreement with the literature data.[20−22] The Ag monolayer causes a complete inhibition of O_2 reduction since only the currents associated with the UPD process are seen in the upper curve. The Ag bilayer also at potentials between 0.65 and 0.75 V inhibits the reaction. A multilayer Ag deposition limits the potential excursions to 0.65 V. The observed inhibition is not surprising, given the very negative potentials of the reaction on bulk silver. In acid solutions, O_2 reduction on Ag starts at $\sim$ 0.3 V, which is considerably more negative than the reaction on Pt(111). O_2 reduction involves a four-electron reduction on bulk Ag,[23] exhibiting a small structural dependence.[24] On a Ag monolayer, in solution containing no Ag^+ ions, O_2 reduction starts at a potential $\sim$0.25 V. A small difference in the activity of bulk Ag and Ag monolayer on Pt(111) is probably a consequence of the different electronic properties of these two surfaces.[25] In addition to O_2 reduction, different catalytic properties of these two surfaces were observed for CO oxidation and sulfate/bisulfate adsorption.[26]

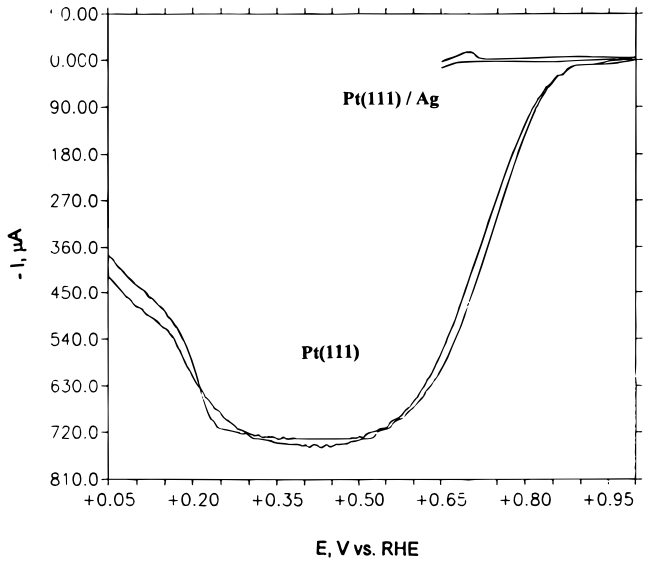

Figure 5. O_2 reduction on a rotating hanging meniscus Pt(111) (lower curve at 0.05 V < E > 1 V), and Pt(111) with Ag monolayer (at 0.75 V < E > 1 V) and Ag bilayer (at 0.65 V < E > 1 V) in O_2-saturated 0.05 M H_2SO_4 with 1 mM Ag^+. Rotation rate: 900 rpm; sweep rate: 50 mV/s; disk area 0.28 cm^2.

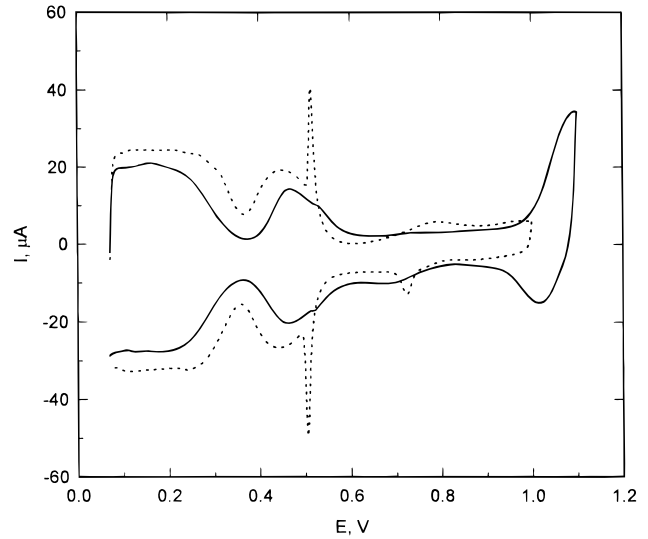

Figure 6. A determination of Ag coverage on Pt(111) in 0.05 M H_2SO_4 from the inhibition of H adsorption in the absence of Ag^+. Curve for Pt(111) without Ag is given by the dashed line. Sweep rate: 20 mV/s.

Measurements of the inhibition of O_2 reduction by Ag adatoms were carried out with Pt(111) as a function of the Ag coverage in the absence of Ag^+ ions in solution. Ag was adsorbed by exposing the Pt(111) crystal to N_2-saturated solutions containing various concentrations of Ag^+ for short time periods. The Ag coverage was determined from the blocking of hydrogen adsorption it causes on Pt(111) which was measured in a separate cell (Figure 6). This procedure permits a determination of the Ag coverage with accuracy better than 4%, and the curves in Figure 6 were reproducibly obtained. The measurements of O_2 reduction were carried out following this determination of the Ag coverage. Since precise determination of the Ag coverage is critical for the analysis of the inhibition effect, the stripping of Ag after O_2 reduction measurement served as a "post-experiment" check. When the two ways of determining Ag coverage yielded the same values, the results of O_2 reduction were taken into consideration. The O_2 reduction as a function of the Ag coverage is shown in Figure 7. A large

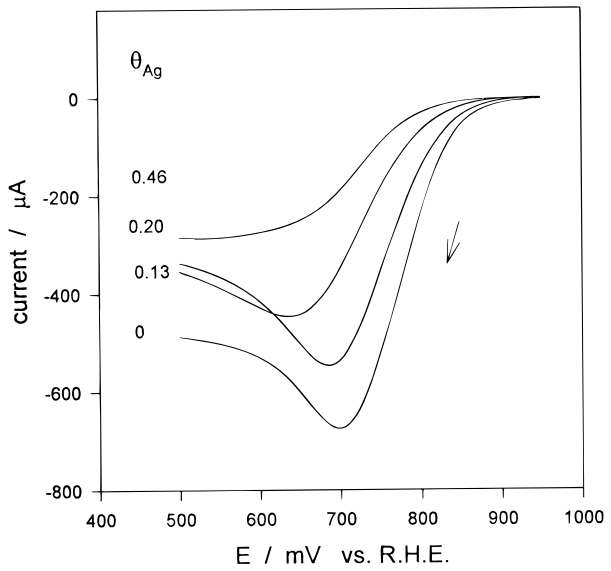

Figure 7. O_2 reduction on a stationary Pt(111)/Ag electrode surface in O_2-saturated 0.05 M H_2SO_4 as a function of Ag coverage. Sweep rate 20 mV/s; disk area 0.78 cm^2.

decrease of the O_2 reduction current at small Ag coverages is seen.

Models of the Site Blocking for O_2 Adsorption by Ag Adatoms. The essential first step in electrocatalytic O_2 reduction is its adsorption on the electrode surface, M, viz.,

$$O_2 + M = M{-}O_2(ads) \qquad (1)$$

The absence of this step would preclude O_2 reduction unless the reaction occurs by an outer sphere charge transfer. (The lack of O_2 reduction currents on the Ag/Pt(111) surface shows that the outer-sphere charge transfer is not operative in this potential region.) It is often assumed that the O_2 adsorbs in a bridge configuration on Pt since it is conducive to a splitting of the O_2 molecule and the ensuing four-electron reduction.[27] There is, however, no spectroscopic method currently available to provide in situ information on O_2 adsorption. It is shown below how the inhibition by Ag adatoms can provide information on this subject, which is of a considerable importance for oxygen electrocatalysis. The use of metal adatoms as a probe of adsorption processes was demonstrated earlier.[28,29]

To gain information on the type of O_2 adsorption on the Pt(111) electrode surface in reaction 1, a model of the site exclusion by Ag atoms is needed. The pronounced inhibition observed indicates that all the Pt atoms interacting with Ag adatoms must be affected and unavailable for bonding because of the changed electronic properties. This conclusion is corroborated by gas-phase data that indicate a charge transfer and redistribution between d and sp electron orbitals of Pt and Ag.[30]

Figure 8 shows models for the site blocking by one Ag atom for adsorption of O_2. For this analysis we took into account, not only on-top and bridge models for O_2 adsorption suggested previously (Figure 1), but also the adsorption in hollow sites. Besides the end-on configuration, O_2 is allowed to adsorb positioned "flat" in two orientations. The Ag adatoms are allowed to adsorb in the 3-fold symmetry hollow sites, as suggested by the SXS data for the Ag monolayer, and also at on-top, and on bridge sites. The models show the Ag adatoms adsorbed on-top block 1, 2, and 3 sites for O_2 adsorbed end-on, at bridge and at hollow sites, respectively (Figure 8a,d,g). The Ag adatoms adsorbed at bridge sites block 2, 3, and 5 sites

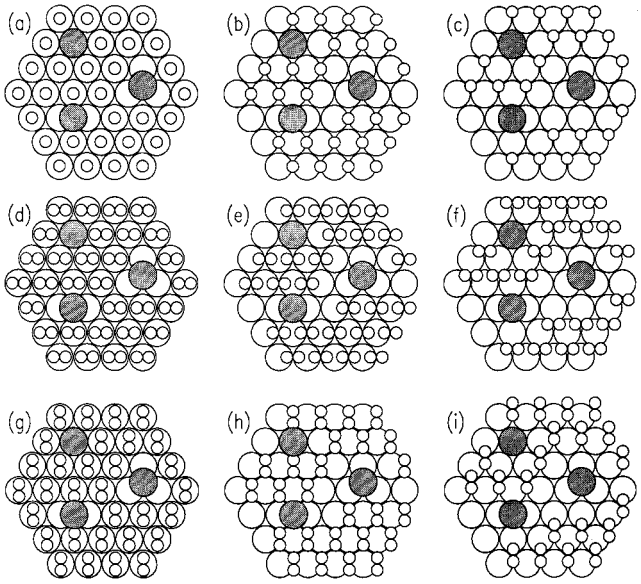

Figure 8. Model of the site-exclusion by Ag atoms adsorbed on top, at bridge and hollow sites for O_2 adsorption at the same sites in three different configurations. Small and large open, and shaded circles represent O, Pt, and Ag atoms, respectively.

(Figure 8b,e,h), while Ag exerts the most effective blocking when adsorbed in hollow sites. These atoms block 3, 5, and 7 sites for O_2 adsorption (Figure 8c,f,i). For example, for the Ag atom adsorbed in the hollow site, which blocks five bridge sites for O_2 adsorption, five 3-fold symmetry sites for Ag adsorption have to be unoccupied to form an ensemble of Pt atoms for the adsorption of one O_2 molecule at the bridge site. Likewise, three hollow sites have to be free from Ag for the adsorption of O_2 at the top site. Protopopoff and Marcus[31] analyzed a range of possible effects of adsorbed sulfur on H_2 adsorption and evolution using a similar approach.

This system can be treated quantitatively by using a simple statistical approach. If n is the number of O_2 sites blocked by one adsorbed Ag atom, an O_2 molecule can adsorb at a particular site only if n Ag sites are not occupied by Ag adatoms. The number of distinguishable ways in which q indistinguishable single particles are arranged on a lattice of N equivalent sites is given by,[32,33]

$$W(q,N) = \binom{N}{q} = N!/(N-q)!\,q! \qquad (2)$$

For example, for O_2 adsorption on bridge sites and Ag adsorption on hollow sites, the ensemble of Pt sites, which has to be unoccupied by Ag in order for O_2 to adsorb, in a bridge position occurs $\binom{N-5}{q}$ times, since on the remaining $(N-5)$ hollow sites, q indistinguishable Ag atoms must be arranged. The probability of having such a structure is

$$P = \binom{N-5}{q} \Big/ \binom{N}{q} \qquad (3)$$

By defining the Ag coverage to be $\theta = q/N$, and assuming N is very large, the equation results in a simple expression $P = (1-\theta)^5$. For the case of on-top O_2 adsorption, the corresponding function is $(1-\theta)^3$. Since the O_2 reduction current is proportional to P, then some models can be distinguished by analyzing the current for O_2 reduction as a function of the Ag coverage.

The plot of the normalized current for O_2 reduction on Pt(111) as a function of the Ag coverage at three different potentials is given in Figure 9. In addition, the curves calculated from the

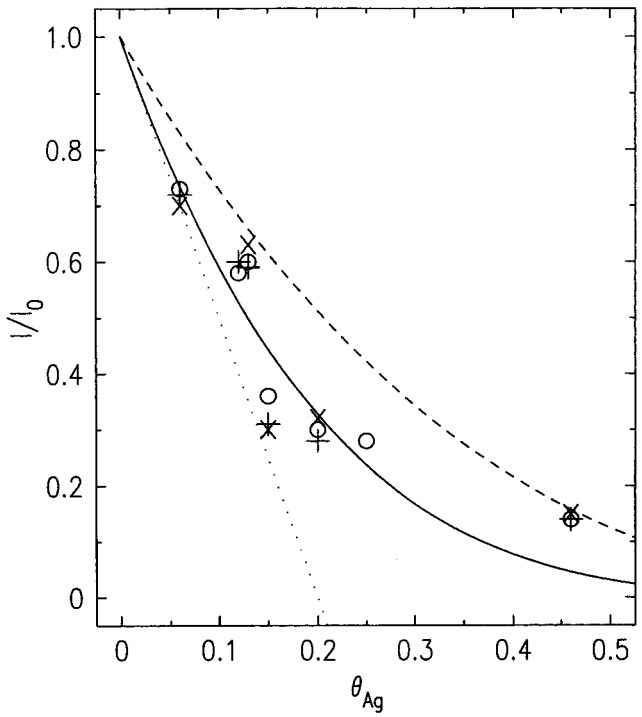

Figure 9. Normalized O_2 reduction current on a stationary Pt(111) electrode as a function of Ag coverage at three potentials (points); calculated curves for the $(1 - \theta)^5$ (solid line) and for the $(1 - \theta)^3$ dependences (dashed line). See text for details.

TABLE 1: Number of Adsorption Sites *n* Excluded for O_2 Adsorption on Pt(111) by Ag Atoms

	n								
O_2 sites	top			bridge			hollow		
O_2 orientations	end-on	⟨1,0⟩	⟨1,2⟩	end-on	⟨1,0⟩	⟨1,2⟩	end-on	⟨1,0⟩	⟨1,2⟩
Ag sites									
top	1	1	1	2	2	2	3	3	3
bridge	2	2	2	3	3	3	5	5	5
hollow	3	3	3	5	5	5	7	7	7

above expressions for the two models of O_2 adsorption configurations are also given. It is seen that for small Ag coverages, up to $\theta_{Ag} \sim 0.26$, the experimental data are in good agreement with the model calculation giving the $(1 - \theta)^5$ dependence. This result can be obtained with Ag adsorbed in hollow sites and O_2 adsorbed on bridge sites (Figure 8 and Table 1). Which of the three O_2 configurations shown in Figure 8b,e,h is operative cannot be distinguished based on this type of analysis. In addition, the adsorption of Ag on a bridge site, with O_2 adsorbed in a hollow site, can produce the same inhibition effect (Figure 8f). The inhibition effect of Ag in hollow sites for O_2 adsorbed also in hollow sites is the highest, i.e., it has the $(1 - \theta)^7$ dependence. Such a large decrease in the O_2 reduction current is not observed experimentally. The adsorption of Ag on bridge sites is energetically less favored than the adsorption in hollow sites. More importantly, in situ SXS data show that in a monolayer coverage Ag is in hollow site (vide supra). It is very unlikely that Ag adsorbs at two different sites at low and high coverage, and the bridge adsorption is probably negligible. Therefore, it can be concluded that most probably O_2 adsorbs at bridge sites on the Pt(111) electrode surface (Figure 8b,e,h). As indicated above, a distinction between three orientations of O_2 at bridge sites cannot be made. However, the end-on configuration (Figure 8b) is not conducive to a 4e-reduction of O_2, but rather to a formation of H_2O_2 in a 2e-reduction. Since the latter is not observed, this configuration appears less plausible than the other two. The molecular orbital calculations for this system of Chan et al.[8] consider the O_2 orientation shown in eq 8e for bridge adsorption. It was found more probable than adsorption at on-top or on hollow sites. The bridge adsorption is also in agreement with the data for adsorption of O_2 on Pt(111) at the metal−gas interface.[6]

A deviation of the experimental data from the calculated curve at the Ag coverages larger than 0.26 is likely due to the island formation during the further growth of the Ag adlayer. The above model is not applicable for such growth, which would cause a close to linear dependence of the inhibition on the Ag coverage. A small difference in the magnitude of inhibition at different potentials for the same Ag coverage may have two causes. First, a small generation of H_2O_2 in a 2e-reduction of O_2 at some step sites affected by Ag will be enhanced at higher overpotentials. H_2O_2 is likely to diffuse to the Pt sites not covered by Ag. That can case an additional small decrease of the O_2 reduction current.

Conclusions

The analysis of the inhibition of O_2 reduction on Pt(111) by silver adatoms indicates that the most probable adsorption of O_2 on Pt(111) electrode surface is a bridge site with an O_2 molecule oriented flat between two Pt atoms. This conclusion, although indirectly, offers an answer to a long-standing question of oxygen electrocatalysis. It also gives a strong support for the views that a 4e-reduction is preceded by splitting of the oxygen−oxygen bond.[3,4] The use of foreign metal adatoms as a probe of adsorption reactions at electrode surfaces now appears to be quite an attractive procedure, provided that the structure of the adsorbate is known as discussed above. The data illustrate the usefulness of the in situ structural information in determining one of the key questions of electrocatalysis − the relationship between the surface structure and its activity.

Acknowledgment. The authors thank S. Feldberg for useful discussions. This research was performed under the auspices of the U.S. Department of Energy, Chemical Sciences and Materials Sciences Division, Office of Basic Energy Sciences under Contract DE-AC02-98CH10886.

References and Notes

(1) Griffith, J. S. *Proc. R. Soc. London, Ser. A* **1956**, *235*, 23.
(2) Pauling, L. *Nature* **1964**, *203*, 182.
(3) Yeager, E. *J. Electrochem. Soc.* **1981**, *128*, 160 C.
(4) Yeager, E.; Razaq, M.; Gervasio, D.; Razaq, A.; Tryk, D. In *Structural Effects in Electrocatalysis and Oxygen Electrochemistry*; Scherson, D., Tryk, D., Daroux, M., Xing, X., Eds.; The Electrochemical Society Inc.: Pennington, NJ, 1992; P. V. 92-11, p 440.
(5) Puglia, C.; Nilsson, A.; Hernnais, B.; Karis, O.; Bennich, P.; Martensson, N. *Surf. Sci.* **1995**, *342*, 119.
(6) Steininger, H.; Lehwald, S.; Ibach, H. *Surf. Sci.* **1982**, *123*, 1.
(7) Outka, D. A.; Stohr, J.; Jark, W.; Stevens, P.; Solomon, J.; Madix, R. J. *Phys. Rev. B* **1987**, *35*, 4119.
(8) Chan, A. W. E.; Hoffmann, R.; Ho, W. *Langmuir*, **1992**, *8*, 1111.
(9) El Omar, F.; Durand, R.; Faure, R. *J. Electroanal. Chem.* **1984**, *160*, 385.
(10) Kamizuka, N.; Itaya, K. *Faraday Discuss.* **1992**, *94*, 117.
(11) Rodriguez, J. F.; Taylor, D. L.; Abruna, H. D. *Electrochim. Acta* **1993**, *38*, 235.
(12) Adžić, R. R. In *Advances in Electrochemistry and Electrochemical Engineering*, Vol. 13; Gerischer, Tobias, C., Eds.; John Wiley: New York, 1984; p 159.
(13) Lucas, C. A.; Markovic, N. M.; Ross, P. N. *Phys. Rev. B* **1997**, *56*, 3651.
(14) Abe, T.; Swain, G. M.; Sashikata, K.; Itaya, K. *J. Electroanal. Chem.* **1995**, *182*, 73.
(15) Wang, J. X.; Marinkovic, N. S.; Adžić, R. R.; Ocko, B. M. *Surf. Sci.*, in press.

(16) Wang, J.; Ocko, B. M.; Davenport, A. J.; Isaacs, H. S. *Phys. Rev. B* **1992**, *46*, 10321; Ocko, B. M.; Wang, J.; Davenport, A. J.; Isaacs, H. S. *Phys. Rev. Lett.* **1990**, *65*, 1466.
(17) Cahan, B. D.; Villulas, H. M. *J. Electroanal. Chem.* **1991**, *307*, 263.
(18) Adžić, R. R.; Wang, J. X.; Ocko, B. M. *Electrochim. Acta* **1995**, *40*, 83.
(19) Adžić, R. R.; Wang, J. X. In *Oxygen Electrochemistry*; Adžić, R. R., Anson, F. C., Kinoshita, K., Eds.; The Electrochemical Society Proceedings Series, Pennington, NJ, 1996; PV 95-26, p 61.
(20) Marković, N. M.; Geistarger, H.; Ross, P. N. *J. Phys. Chem.* **1995**, *99*, 3411.
(21) El Kadiri, F.; Faure, R.; Durant, R. *J. Electroanal. Chem.* **1991**, *301*, 177.
(22) Marković, N. M.; Adžić, R. R.; Cahan, B. D.; Yeager, E. B. *J. Electroanal. Chem.* **1994**, *377*, 249.
(23) Fisher, P.; Heitbaum, J. *J. Electroanal. Chem.* **1980**, *112*, 231.
(24) See, e.g., Adžić, R. R. In *Modern Aspects of Electrochemistry*, Vol. 21; p 163, White, R. E., Bockris, J. O'M., Conway, B. E., Eds.; Plenum Press: New York, 1990.
(25) Rodriguez, J. A.; Kuhn, M. *J. Phys. Chem.* **1994**, *98*, 11251.
(26) Marinkovic, N. S.; Marinkovic, J. S.; Wang, J.; Adžić, R. R. *J. Phys. Chem*., submitted for publication.
(27) Yeager, E.; Razaq, M.; Gervasio, D.; Razaq, A.; Tryk, D. *J. Serb. Chem. Soc*. **1992**, *57*, 819.
(28) Adžić, R. R.; Spasojevic, M. D.; Despic, A. R. *Electrochim. Acta* **1979**, *24*, 569.
(29) Adžić, R. R.; Feddrix, F.; Nikolic, B. Z.; Yeager, E. *J. Electroanal. Chem.* **1992**, *341*, 287.
(30) Rodriguez, J. A.; Kuhn, M. *J. Phys. Chem.* **1994**, *98*, 11251.
(31) Protopopoff, E.; Marcus, P. *J. Chim. Phys*. **1991**, *88*, 1423.
(32) Miyazaki, E.; Yasumori, I. *J. Math. Phys*. **1977**, *18*, 215.
(33) Martin, G. A. In *Metal-Support and Metal-Additives Effects in Catalysis*; Imelik, B., et al., Eds.; Elsevier: Amsterdam, 1982.